

SIMULATION OF FLUID-STRUCTURE INTERACTION IN AN ARTERY ALTERED BY SEGMENTAL MEDIOLYSIS

Mouloud Mohellebi^{1*}  [0009-0003-2657-6243], Mohamed Ferrouk¹  [0000-0003-4184-2899] and Hocine Tebbiche¹  [0000-0002-5151-9625]

¹ Laboratoire d'Energétique, Mécanique et Matériaux, Université Mouloud Mammeri de Tizi Ouzou, 15000 Tizi Ouzou, Algeria

**corresponding author*

Abstract

Segmental arterial mediolysis (SAM) is an asymptomatic, non-atherosclerotic and non-inflammatory disease of unknown etiology. It affects medium-sized arteries and is characterized by vacuolization and lysis at the level of the media which can lead to dissection, steno-occlusion, or an aneurysm. In this article, a simulation of fluid-structure interaction in an artery altered by segmental mediolysis was reported. The study showed that the reduction in elasticity of the media layer of the artery due to the deterioration of collagen has little influence on the velocity field, the pressure field as well as on the deformations of the artery, thus conferring a silent and asymptomatic character to the pathology. The Von-Mises stress is very high at the level of the intima which can lead to arterial dissection with the appearance of a false channel. An increase in the Von-Mises stress of around 375 % was predicted by the COMSOL code. The combined effect of mediolysis and the increase in blood pressure causes increases in the Von-Mises stress at the level of the intima and the adventitia which are respectively 6.10 and 4.62 times greater than those of the healthy artery, which demonstrates that hypertension could be a determining factor in triggering arterial dissection.

Keywords: Artery, dissection, media, Von-Mises stress.

1. Introduction

Segmental arterial mediolysis (SAM) is a disease with a serious manifestation and unknown etiology, affecting medium-sized arteries. It causes arterial dissection and qualifies as a medical emergency. The disease was initially named segmental medial arteritis (Slavin et al. 1976) and following the observation of the pathological process different from that of arteritis, it was renamed MAS (Slavin et al. 1995). SAM is manifested by the degradation of the mechanical properties of the median layer of the artery that can lead to dissection, steno-occlusion, or aneurysm (Gaud et al. 2010, Tehrany et al. 2017). According to Skeik et al. (2019), the disease generally affects middle-aged adults and can, in some cases, cause major complications leading to death. Given the asymptomatic and silent nature of SAM, recommendations for diagnosis and appropriate management were given by Skeik et al. (2019) by favoring a conservative strategy. However, further research is needed to standardize diagnostic criteria and establish an appropriate consensus for management. Currently, according to Kennedy et al. (2021), there is no

standardized guideline for the management of SAM patients due to the lack of randomized controlled trials. In order to reduce the cardiovascular risk profile, the authors emphasize the need for lifestyle changes, control of hypertension and dyslipidemia.

Several researchers, (Van Bordel, 2006; Danpinid et al., 2010) investigated arterial pathologies and claimed that changes in the mechanical properties of the middle layer (media) arteries are at the origin of the appearance of several arterial pathologies for which variation in rigidity is considered as an indicator of their appearance. The measurement of rigidity based on the Windkessel model proposed by O'Rourke et al. (2002) is very limited for a complete explanation of arterial behaviour; nevertheless, in certain specific circumstances, such as in very old people with diagnosed hypertension it may seem realistic. Using data from a multi-slice 64-CT scanner and creating software for finite element mesh manipulation and post-processing, Milašinović et al. (2008) simulated and represented velocity profiles and distributions of the effect of velocity and wall stress for two models of aortic geometries with and without aneurysm and under systolic and diastolic flow conditions. The multidisciplinary approach validated by these authors has made it possible to offer new perspectives to clinical investigation by developing computer simulation tools.

The work of L. de Figueiredo Borges et al. (2008) showed that the decrease of collagen in the media is responsible for aortic dissection and aneurysms, and the localization of this decrease is mainly in the external part of the media in the case of dissection while in the case of aneurysms, it is more diffuse in coherence with the global enlargement. Khanafer et al. (2009) found that the median layer with the largest modulus of elasticity had the highest Von-Mises stress. For different ratios of thickness (13/56/31) and elasticity (2/6/4MPa) of aortic walls with Newtonian and turbulent blood flow, the numerical results of the simulation of the behaviour of the fluid structure interaction showed that the appearance of a dissection in the media layer is due to the difference in the elastic properties of the three layers of the aorta.

Two invasive treatment methods, namely, stented aneurysm and polytetrafluoroethylene (PTFE) wrapped aneurysm, were compared by Gao et al. (2013). The comparison was conducted using the COMSOL multiphysics computational code by focusing on the behaviour of the fluid-structure interaction. According to Gao et al. (2013), the maximum Von Mises stress of the stent model is reduced by about 37 % in the wrapped aneurysm model. These results are of great importance for the understanding of the biomechanics of stenting and the envelopment of aneurysmal arteries. To understand the tearing phase of an aortic dissection, MacLean et al. (1999) studied the response of the thoracic aorta to radial and longitudinal forces and showed that the aorta tears radially at a much lower value of radial tensile stress than would have been predicted by previous studies reporting the longitudinal and circumferential Young's modulus.

This would explain, according to these authors, why dissections propagate easily once the initial tear has occurred. Nevertheless, it should be noted that the tri-layer character of the artery was not taken into consideration. The recent work of Zhu et al. (2023) has shown that CFD combined with 4D MRI provides comprehensive information for predicting the evolution of aortic dissection that goes beyond what can be obtained by anatomical evaluation alone. The information can be used to tailor the treatment to each patient. They were based on the detection of recirculation zones, pressure disturbances and shear stresses at the walls.

In this article, a simulation of the behaviour and explanation of the occurrence of arterial dissection during the deterioration of collagen in the middle layer of the artery using the COMSOL multiphysics software is reported. The effect of the elastic modulus of the media segment on Von-Mises stress was studied. The simulation also showed that the presence of this pathology has a very small influence on the velocity field, the pressure field as well as on the displacements of the artery. This would explain the asymptomatic and silent character of this

arterial dissection constituting a danger of death. The case of the combination of media weakening and increased blood pressure was also addressed in this study.

2. Mathematical formulation

The Navier-Stokes equations governing flow are simplified using the symmetry property. In internal flows, rotational symmetry about the conduit axis is most often encountered, but in a number of circumstances the assumption of two-dimensional plane flow provides a good representation of the actual situation. The equations governing wall displacement are established for a thin-walled, elastic conduit.

2.1. Flow equations

The continuity and momentum equations, using a cylindrical polar coordinate system for steady incompressible isothermal flow are given, following Ward-Smith (1980):

$$\frac{\partial u}{\partial x} + \frac{1}{r} \frac{\partial}{\partial r}(rv) = 0 \quad (1)$$

$$u \frac{\partial u}{\partial x} + v \frac{\partial u}{\partial r} = -\frac{1}{\rho_f} \frac{\partial p}{\partial x} + \nu \left[\frac{1}{r} \frac{\partial}{\partial r} \left(r \frac{\partial u}{\partial r} \right) + \frac{\partial^2 u}{\partial x^2} \right] \quad (2)$$

$$u \frac{\partial v}{\partial x} + v \frac{\partial v}{\partial r} = -\frac{1}{\rho_f} \frac{\partial p}{\partial r} + \nu \left[\frac{1}{r} \frac{\partial}{\partial r} \left(r \frac{\partial v}{\partial r} \right) - \frac{v}{r^2} + \frac{\partial^2 v}{\partial x^2} \right] \quad (3)$$

where the x-axis is selected to coincide with the axis of artery and radial coordinate is denoted by r. In a dimensionless form, we obtain:

$$\frac{\partial u_N}{\partial x_N} + \frac{1}{r_N} \frac{\partial}{\partial r_N}(r_N v_N) = 0 \quad (4)$$

$$u_N \frac{\partial u_N}{\partial x_N} + v_N \frac{\partial u_N}{\partial r_N} = -\frac{1}{\rho_f U_1^2} \frac{\partial p}{\partial x_N} + \frac{2}{\text{Re}} \left[\frac{1}{r_N} \frac{\partial}{\partial r_N} \left(r_N \frac{\partial u_N}{\partial r_N} \right) + \frac{\partial^2 u_N}{\partial x_N^2} \right] \quad (5)$$

$$u_N \frac{\partial v_N}{\partial x_N} + v_N \frac{\partial v_N}{\partial r_N} = -\frac{1}{\rho_f U_1^2} \frac{\partial p}{\partial r_N} + \frac{2}{\text{Re}} \left[\frac{1}{r_N} \frac{\partial}{\partial r_N} \left(r_N \frac{\partial v_N}{\partial r_N} \right) - \frac{v_N}{r_N^2} + \frac{\partial^2 v_N}{\partial x_N^2} \right] \quad (6)$$

where

$$u_N = \frac{u}{U_1}, v_N = \frac{v}{U_1}, x_N = \frac{x}{R}, r_N = \frac{r}{R}, \text{Re} = \frac{2RU_1}{\nu}$$

2.2. Wall motion equations

On the hypothesis of an artery with a thin elastic wall, of thickness e, density ρ_a , modulus of elasticity E, Poisson's ratio σ , calling ξ the radial displacement of a point on the wall and η its axial displacement, the equations of wall motion are given, following Comolet (1974):

$$\rho_a e \frac{\partial^2 \xi}{\partial t^2} = p - \tau_{rr} - \frac{Ee}{1 - \sigma^2} \left(\frac{\sigma}{R} \frac{\partial \eta}{\partial x} + \frac{\xi}{R^2} \right) \quad (7)$$

$$\rho_a e \frac{\partial^2 \eta}{\partial t^2} = \tau_{rx} + \frac{E e}{1 - \sigma^2} \left(\frac{\partial^2 \eta}{\partial x^2} + \frac{\sigma}{R} \frac{\partial \xi}{\partial x} \right) \quad (8)$$

where τ_{rr} and τ_{rx} are the viscous stresses applied by the fluid to the wall at $r = R + \xi$:

$$\tau_{rr} = 2\mu \frac{\partial v}{\partial r}, \tau_{rx} = \mu \left(\frac{\partial u}{\partial r} + \frac{\partial v}{\partial x} \right)$$

3. Boundary conditions, grid model, and numerical method

The reference data in this study refer to a medium-diameter vessel published by Comolet (1974). The vessel's internal diameter and length are 5 mm and 150 mm, respectively. The vessel is assumed to be cylindrical, deformable and composed of three distinct concentric layers (Fig. 1), which are, from the inside to the outside: intima, media and adventitia, having respective thicknesses of 0.08 mm, 0.5 mm and 0.25 mm. The elastic moduli of each of these layers for a healthy artery are respectively 2MPa, 6MPa and 4MPa with a Poisson modulus of 0.45 and a density of 960 kg/m³. The media layer presents, at its mid-length on a segment of length 50 mm, an axisymmetric alteration (Fig. 1) resulting in a reduction in the modulus of elasticity following the deterioration of collagen.

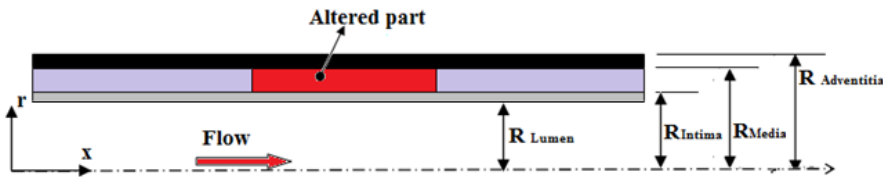


Fig. 1. Locally altered tri-layer vessel diagram

The boundary conditions used in this study are those corresponding to the normal physiological values (without hypertension) in the case of systolic peak (maximum values of pressure and velocity). The fluid and wall equations are coupled to the wall by the wall adhesion condition and are solved using the COMSOL code for the following boundary conditions:

$$x = 0, u = U_1 = 0.1 \text{ m/s for all } r$$

$$x = L, p = 15900 \text{ Pa for all } r$$

$$r = R, u = 0 \text{ for all } x$$

$$r = 0, \partial u / \partial r = 0 \text{ for all } x$$

For the wall, several conditions were considered: a condition of free movement at the fluid-structure interface, a condition of free axial and radial movement and finally a condition of embedding for the ends. A mapped quadrilateral mesh was used for the different domains. The mesh independence was checked for different mesh numbers. The calculations showed that the maximum difference in Von-Mises stress and wall displacements does not exceed 2.5 % between coarse and fine meshes. Figures 2 and 3 show the sensitivity and evolution of the Von-Mises stress and radial displacement as a function of the number of elements. The fine mesh retained for our calculations, uses 6750 meshes for the fluid domain and for the solid domain, made up of intima, media and adventitia, 1350, 5400 and 2700 meshes respectively. This same mesh was adopted for the reference data reported by Khanafer et al. (2009) for an aorta characterized by the following dimensions: $R_{\text{lumen}}=12$ mm, $R_{\text{intima}}=12.2$ mm, $R_{\text{media}}=13.4$ mm and $R_{\text{adventitia}}=14$ mm.

The numerical results that follow, regarding the effect of elasticity on Von-Mises stress during systolic peak, agree very well with those presented by Khanafer et al. (2009).

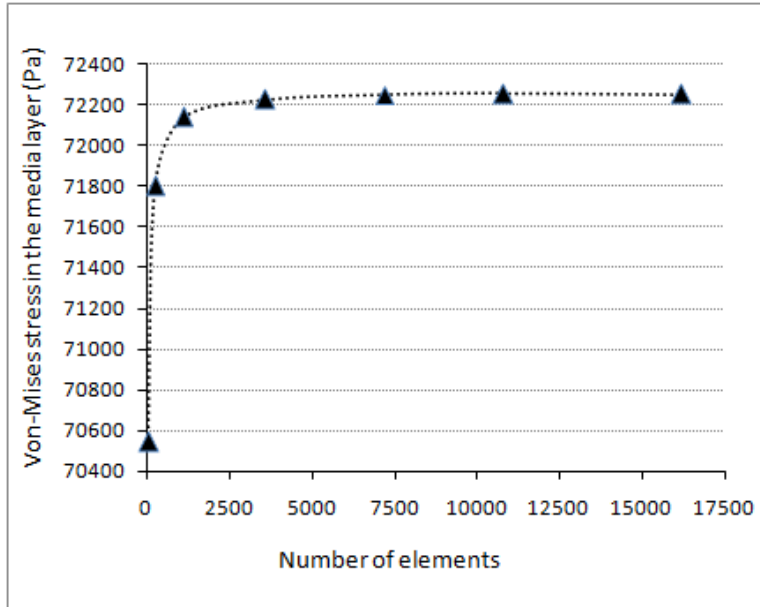


Fig. 2. Von-Mises stress in the media layer as a function of the number of meshes

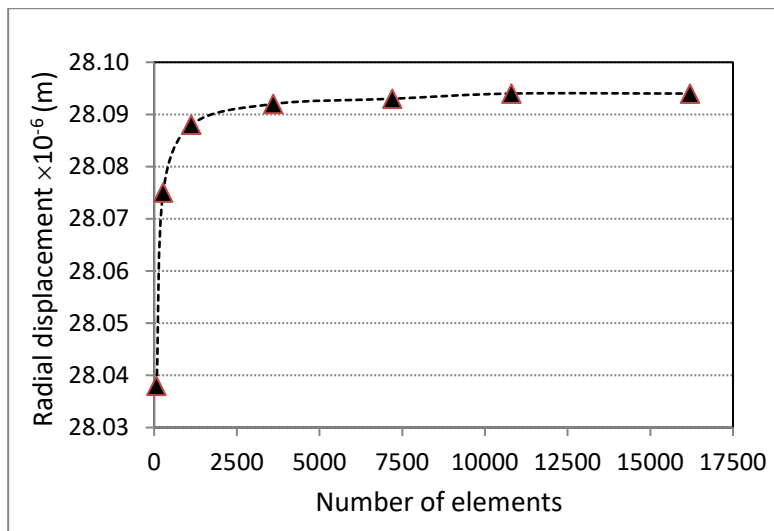


Fig. 3. Radial displacement of the intima wall as a function of the number of meshes

4. Results and discussion

Simulations of the behaviour and explanation of the occurrence of arterial dissection during the collagen deterioration at the media layer using the COMSOL multiphysics code were performed.

Parietal deformations induced by hemodynamic conditions and collagen deterioration were determined. The effect of reducing elasticity due to age, environment and genetic factors, has been studied.

The presented results have been calculated, considering the systolic peak conditions where the pressure and velocity are maximum and the elasticity of the media layer in the altered part has been reduced from a value of 6 MPa to a value of 0.1 MPa corresponding to the state of deterioration.

4.1. Effect of the modulus of elasticity of the altered part on velocity

The parabolic profile of velocities at the altered portion of the artery is shown in Fig. 4. The profile along the vessel is very weakly affected by the presence of the altered portion. At the location of the alteration, Fig. 5 shows the variation of the velocity along the conduit and Fig. 6 represents the rate of variation of this velocity along the conduit by reducing the modulus of elasticity of 6 MPa of a healthy artery to 0.1 MPa of an artery with mediolytic. A drastic reduction in elasticity (of the order of 98 %) only causes a 7.5 % reduction in velocity. This gives the pathology a character difficult to detect and appreciable by ultrasonic velocimetry.

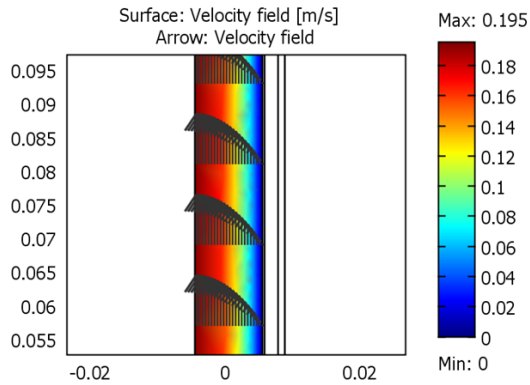


Fig. 4. Velocity profile in the artery with alteration of the media

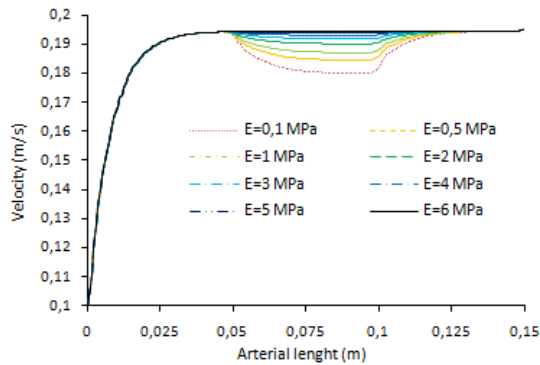


Fig. 5. Velocity variation depending on the modulus of elasticity of the altered part

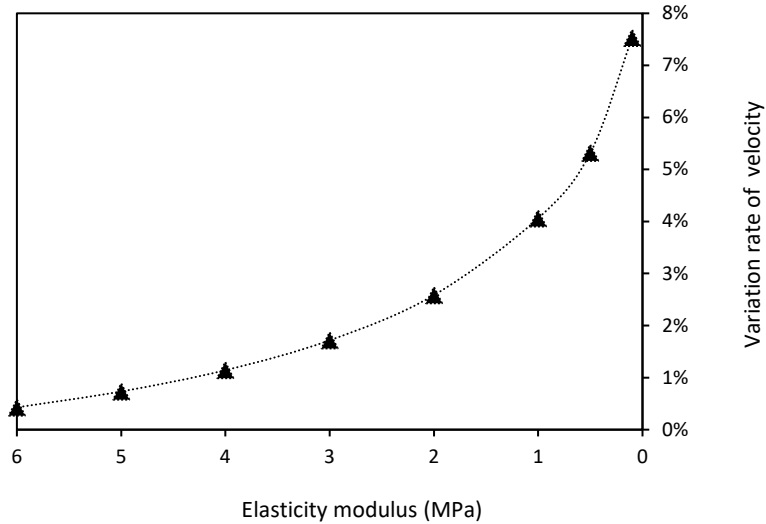


Fig. 6. Rate of change of velocity at the altered part

4.2. Effect of the modulus of elasticity of the altered part on pressure

Figure 7 shows the evolution of the pressure along the artery. The decrease of the modulus of elasticity makes the artery more deformable and causes swelling in the altered part. Fig. 8 shows the radial displacement of the artery radius as a function of the modulus of elasticity. The radial unit deformation is shown in Fig. 9 and is of the order of 5 % for the lowest value of the modulus of elasticity. The increase in the inner radius of the artery leads to a decrease in the resistance of Poiseuille and therefore the loss of charge. In the laminar mode, the latter is proportional to the flow rate and inversely proportional to the fourth power of the radius. In our fluid -structure simulation, downstream pressure is kept constant resulting in lower pressure in the artery entrance area as shown in Fig. 7. Small decreases in pressure and rate of radius displacement compared to the initial dimensions of the artery make it difficult to diagnose the pathology of segmental arterial mediolysis.

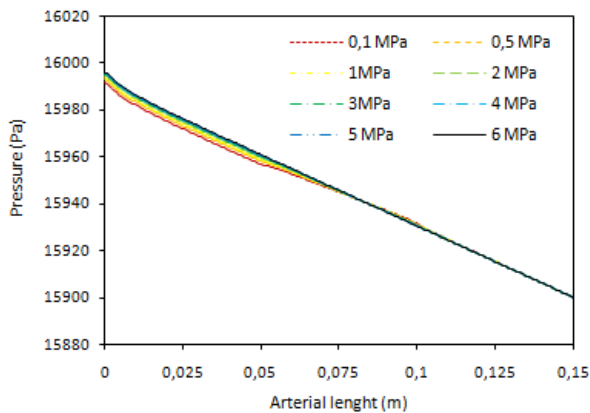


Fig. 7. Pressure variation along the artery

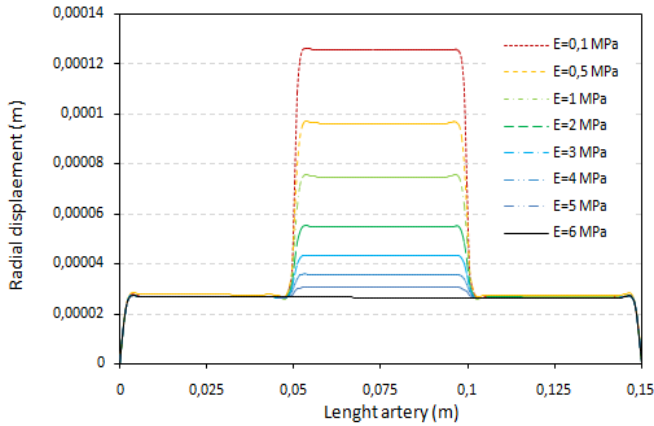


Fig. 8. Radial displacement of the inner wall for different values of the modulus of elasticity

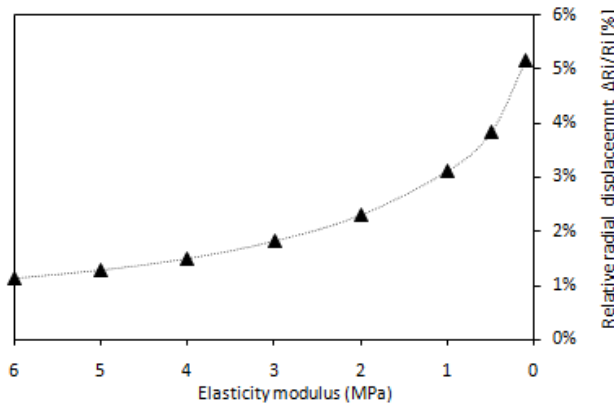


Fig. 9. Unitary radial deformation at the middle of the artery

4.3. Effect of the modulus of elasticity on Von-Mises stresses

In order to predict the rupture of the artery due to the reduction of the modulus of elasticity caused by the mediolysis, the Von-Mises criterion was evaluated. Indeed, the theory predicts that a material begins to yield when the Von-Mises stress reaches a level equal to the limit stress.

The Von-Mises stress predicted by the COMSOL code in the middle of the conduit where the altered part of the media is located is represented in Fig. 10 as a function of the artery radius and for the two limit values of the modulus of elasticity. As shown in Fig. 10, the Von-Mises stress increases considerably at the intima and adventitia and decreases at the media with the reduction of the modulus of elasticity. The significant increase in Von-Mises stress for intima and adventitia is 375 % and 310 %, respectively. While for media, the reduction of the modulus of elasticity, from 6 MPa to 0.1 MPa, results in a 92 % decrease in Von-Mises stress. Figure 11 shows the evolution of the Von-Mises stress as a function of the media elasticity modulus at the altered part. The adventitia and the intima have the same behaviour with a rate of variation of the Von-Mises constraint almost confused (Fig. 12). The Von-Mises constraint of the media evolves

in the opposite direction of those of the intima and the adventitia and for elasticity modulus less than 2 MPa the gap increases in size.

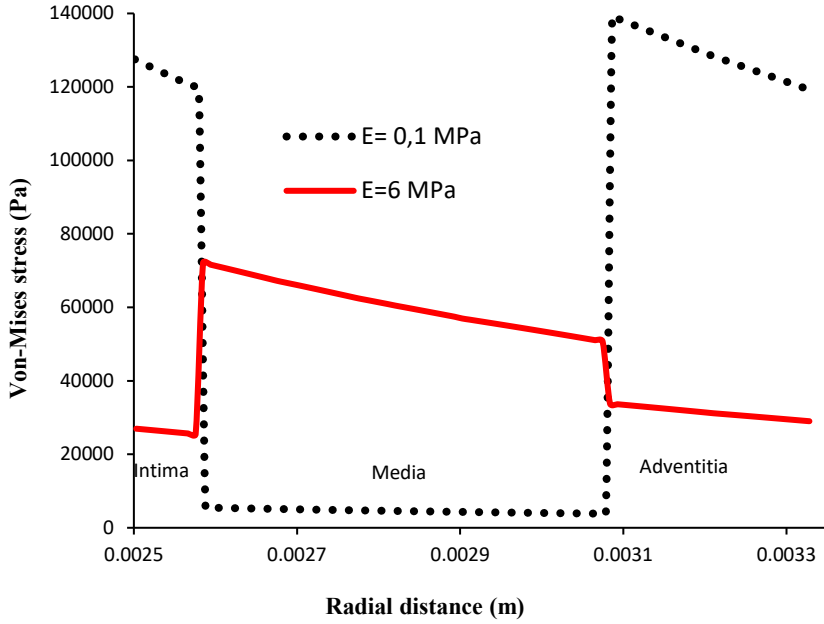


Fig. 10. Evolution of Von-Mises stress in the three layers

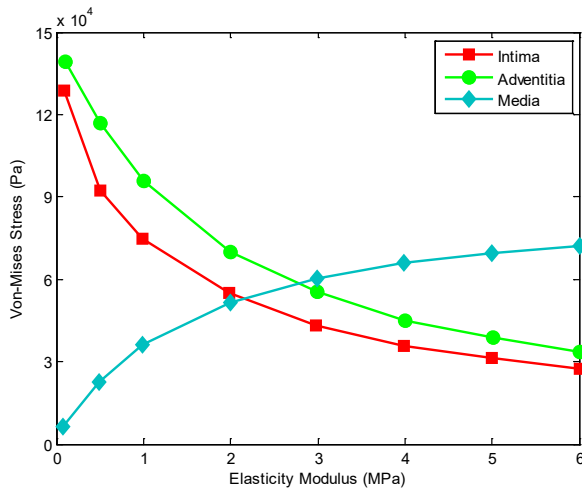


Fig. 11. Evolution of Von-Mises stress as a function of the modulus of elasticity

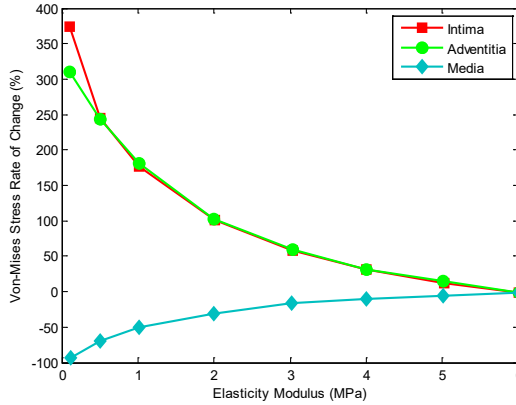
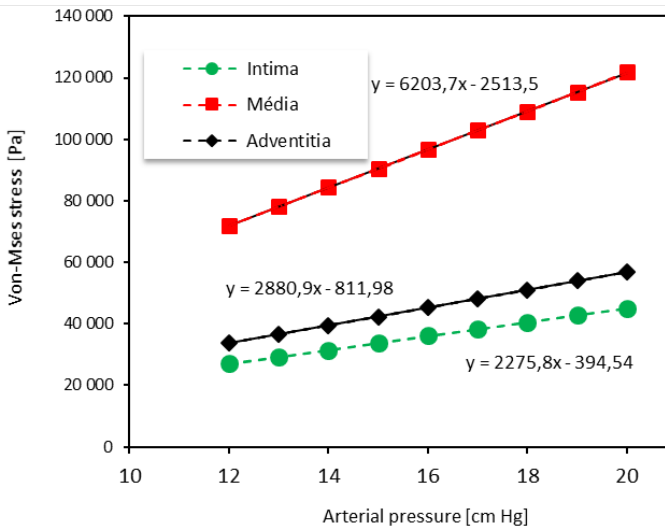


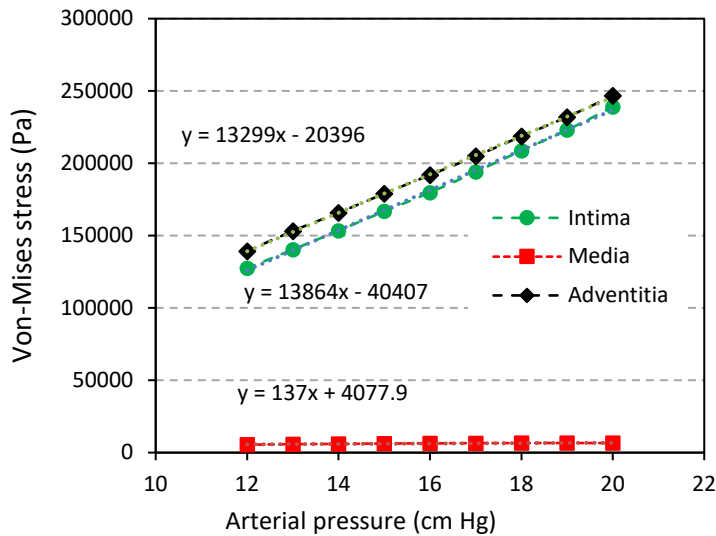
Fig. 12. Von-Mises stress variation rate

4.4. Effect of blood pressure on Von-Mises stress

In accordance with the recommendations of Kennedy et al. (2021), particularly for the control of high blood pressure, the impact of the latter on Von-Mises constraints within the three layers of the artery was analysed. Figure 13 shows that the evolution of the Von-Mises stress evolves linearly with blood pressure. For a healthy artery (Fig. 13a), the maximum stress occurs at the level of the media, the slope of which is 2.72 times greater than that of the intima and 2.15 times greater than that of the adventitia. In the case of the combination of the weakening of the media and the increase in blood pressure (Fig. 13b), the lines of evolution of the Von-Mises stress at the intima and the adventitia are steeper where their slopes are respectively 6.10 and 4.62 times those of the healthy artery. Thus, this demonstrates that hypertension could be a determining factor in triggering arterial dissection.



(a)



(b)

Fig. 13. Evolution of Von-Mises stress in the three layers. (a) Healthy artery; (b) Altered artery

5. Conclusion

The fluid-structure behaviour of an artery affected by segmental arterial mediolysis was studied. The destruction of collagen, an element ensuring the rigidity and stability of the middle layer (media) of the wall, was modelled using the COMSOL Multiphysics code to predict the distributions of pressure, velocity, stress and displacement in the altered portion of the artery. The following important conclusions are therefore drawn:

1. For systolic peak conditions, the variation of the elastic modulus of the media has a very weak influence on the velocity profile, pressure field and wall displacements. The destruction of collagen leading to a reduction in elasticity of the order of 98 % only generates a 7.5 % reduction in velocity and a unitary radial deformation of the order of 5 %. This is what gives this pathology a silent and asymptomatic character.
2. The Von-Mises stress is very high in the intima which can lead to arterial dissection with the appearance of a false channel. An increase in the Von-Mises stress of around 375 % was predicted by the COMSOL code.
3. The combination of mediolysis and high blood pressure leads to rates of variation of the Von-Mises stress at the intima and adventitia higher than those of the healthy artery by 6.10 and 4.62 times thus favouring the appearance of dissection.

Acknowledgements: The authors acknowledge the support of the Ministry of Higher Education and Scientific Research (MESRS) of Algeria, Grant A11N01UN150120220003.

References:

- Comolet R (1974). *Circulatory Biomechanics*, Masson.
- Danpinid A., Luo J., Vappou J., Terdtoon P., Konofagou E. E. (2010). In vivo characterization of the aortic wall stress–strain relationship. *Ultrasonics*, 50(7), 654-665
- De Figueiredo Borges L., Jaldin R. G., Dias R. R., Stolf N. A. G., Michel J. B., Gutierrez P. S. (2008). Collagen is reduced and disrupted in human aneurysms and dissections of ascending aorta. *Human pathology*, 39(3), 437-443
- Gao F., Ueda H., Gang L., Okada H. (2013). Fluid structure interaction simulation in three-layered aortic aneurysm model under pulsatile flow: comparison of wrapping and stenting. *Journal of Biomechanics*, 46(7), 1335-1342.
- Gaud S., Cridlig J., Claudon M., Diarrassouba A., Kessler M., Frimat L. (2010). Segmental arterial medialysis and renal vascular hypertension. *Nephrology & Therapy*, 6(7), 597-601.
- Kennedy C. A., Toomey D. P. (2021). Segmental arterial mediolysis: a rare cause of an acute abdomen. *Journal of Surgical Case Reports*, 2021(10), rjab370.
- Khanafer K., Berguer R. (2009). Fluid–structure interaction analysis of turbulent pulsatile flow within a layered aortic wall as related to aortic dissection. *Journal of Biomechanics*, 42(16), 2642-2648.
- MacLean N. F., Dudek N. L., Roach M. R. (1999). The role of radial elastic properties in the development of aortic dissections. *Journal of Vascular Surgery*, 29(4), 703-710
- Milašinović D., Ivanovic M., Tengg-Kobligk H., Böckler D., Filipović N. (2008). Software tools for generating CFD simulation models of blood flow from CT images, and for postprocessing. *Journal of the Serbian Society for Computational Mechanics*, 2(2), 51-58.
- O'Rourke M. F., Staessen J. A., Vlachopoulos C., Duprez D., Plante G. É. E. (2002). Clinical applications of arterial stiffness; definitions and reference values. *American Journal of Hypertension*, 15(5), 426-444.
- Slavin R. E., Gonzalez-Vitale J. C. (1976). Segmental mediolytic arteritis: a clinical pathologic study. Laboratory investigation; *A Journal of Technical Methods and Pathology*, 35(1), 23-29.
- Slavin R. E., Saeki K., Bhagvan B, Maas A. E. (1995). Segmental arterial mediolysis: a precursor to fibromuscular dysplasia? *Mod Pathol* 8: 287-94
- Skeik, N., Olson, S. L., Hari, G., & Pavia, M. L. (2019). Segmental arterial mediolysis (SAM): systematic review and analysis of 143 cases. *Vascular Medicine*, 24(6), 549-563.
- Tehrany Y. A., Terraz, S., Seebach, P. J. D. (2017). Segmental arterial mediolysis: a differential diagnosis of vasculitis. *Rev Med Switzerland*, 13, 754-7.
- Van Bortel L. M. (2006). Is arterial stiffness ready for daily clinical practice? *Journal of Hypertension*, 24(2), 281-283.
- Ward-Smith A. J. (1980). *Internal fluid flow-The fluid dynamics of flow in pipes and ducts*. Clarendon Press Oxford.
- Zhu, Y., Xu, X. Y., Rosendahl, U., Pepper, J., & Mirsadraee, S. (2023). Advanced risk prediction for aortic dissection patients using imaging-based computational flow analysis. *Clinical Radiology*, 78(3), e155-e165.